Reports

Water Vapor: Stratospheric Injection by Thunderstorms

Abstract. *Infrared radiometric inference measurements of the mass of water vapor injected into the lower stratosphere and upper troposphere by a number of plains thunderstorms show an average threefold increase over the fair weather background mass of water vapor. These airborne measurements, made from the National Aeronautics and Space Administration Convair 990 jet laboratory, extended over a sample size much larger than that possible by balloon and other techniques.*

High-altitude infrared measurements of the total mass of water vapor above flight level in the vicinity of thunderstorms, at and just below the base of the stratosphere, were made in July 1971 over the Central Plains. Observations revealed that the vertical drive of these huge storm cells resulted in the local injection of large amounts of water vapor into the atmosphere. The National Aeronautics and Space Administration (NASA) Ames Research Center's Convair 990 (CV-990) jet laboratory provided the long-range, high-speed, and high-altitude capability required in this study. The purpose of the flight measurements was to determine, in situ, the amount of water vapor transported vertically into the lower stratosphere by a thunderstorm cell or system. A summary of the instrumentation, the numerical treatment, and typical results of the experiments follows.

Infrared inference techniques were used to avoid the difficulty of obtaining satisfactory, uncontaminated samples of water vapor from aircraft with frost-point or wet chemical instrumentation. It was possible to modify the existing on-board (CV-990) radiometer to operate over the 17.5- to 26.32-μm portion of the rotational spectral band of water vapor as a bottom sounder. Bottom-sounding measurements, as opposed to satellite top-sounding measurements, require careful purging of the system with dry nitrogen (*1*). This procedure is necessary because the mass of water vapor above the aircraft is very small, approximately 10^{-4} of the mass above the earth's surface, and contamination from the aircraft cabin must be eliminated. The in-line chopper-bolometer radiometer used exhibited a noise equivalent change in radiance (ε) of 2.00×10^{-6} watt cm^{-2} steradian^{-1} in the spectral interval of measurement. At an altitude of approximately 13.0 km and for a typical July temperature sounding for Denver, this corresponds to a root-mean-square error in the columnar mass of water vapor above 13.0 km measured by infrared techniques of 1.0×10^{-4} g cm^{-2}. The standard error (the root-mean-square error divided by the square root of the number of observations of the same target) is approximately one-tenth of the root-mean-square error. A second infrared channel operating in the 10.0- to 12.0-μm band provided a constant check on the presence of any cloud particles in the path that would negate the values being recorded on the channel being used to measure the mass of water vapor. Self-emission from the KRS-5 (potassium thallium bromoiodide) window, the radiometer 10.0-cm Cassegrain optics, and the exterior mirror system were monitored by strategic location of gold-coated thermistors. The KRS-5 window has a very low emissivity ($\sim$0.02) and is atmospherically cold-soaked at high altitudes to approximately -40°C, thus ensuring a low emission.

An inverse solution of the radiative transfer equation is used to infer the mass of water vapor above a reference plane in the atmosphere. The rapidly converging solution is obtained by iteration (*2*). Briefly, the downward radiance $N_c\downarrow$ is expressed mathematically as

$$N_c\downarrow = -\int_{\nu_1}^{\nu}\int_{\tau=1}^{\tau} B[\nu, T(p)]d\tau\,[p, u(H_2O)]d\nu \qquad (1)$$

where ν is the wave number, τ is the transmissivity, B is the Planck function, T is the temperature, p is the pressure, and $u(H_2O)$ is the mass of water vapor. Since we have a temperature profile directed upward, we can calculate the downward radiance, $N_c\downarrow$, assuming an initial water vapor mass profile. This assumption is one of a constant mixing ratio profile, $\bar{s}(p)$, in grams of water per gram of air. A unique mass of water vapor above the reference level is found by computer calculation of $N_c\downarrow$ such that the difference between the observed and calculated downward radiance, $|N_o\downarrow - N_c\downarrow|$, is minimized. This minimization is accomplished by a conventional iterative method (Newton's) to obtain repeated values of $(N_o\downarrow - N_c\downarrow|$ from successive approximations of $u(H_2O)$.

We summarize the iterative, radiometric inference of the mass of water vapor in the following functional notations:

$$N_o\downarrow = N_o\downarrow(u) \qquad (2)$$

$$N_c\downarrow = N_c\downarrow(\tau) \qquad (3)$$

$$\tau = \tau(u) \qquad (4)$$

$$u = u(\bar{s}) = 1/g)\bar{s}\Delta p \qquad (5)$$

$$\bar{s} = \bar{s}\ \ (|N_o\downarrow - N_c\downarrow| \leq \epsilon) \qquad (6)$$

In Eq. 5 g is the acceleration due to gravity and $\bar{s}$ is the mixing ratio (water vapor to air in parts per million). The use of mean monthly temperature soundings gives "first look" real-time solutions on a small, on-board computer during flight operations.

In all, six isolated thunderstorm cells penetrating the tropopause and two squall-line cell systems were investigated. The difference between the mass of water vapor upstream and that downstream of the storm cell is a measure of the amount of water vapor transported vertically by the thunderstorm, since, on the average, the wind moves through and above the visible top of the storm cell, generally from west to east. It appears logical, then, to look for any addition of water vapor into the upper troposphere and lower stratosphere in a volume translated downstream from the top of the storm cell itself. Since the water vapor is presumably swept along in this wind field, this procedure will ensure measurement of any actual addition of water vapor to the stratosphere or upper troposphere persisting away from the cell.

A typical and interesting reconnaissance of a single cell system is that of

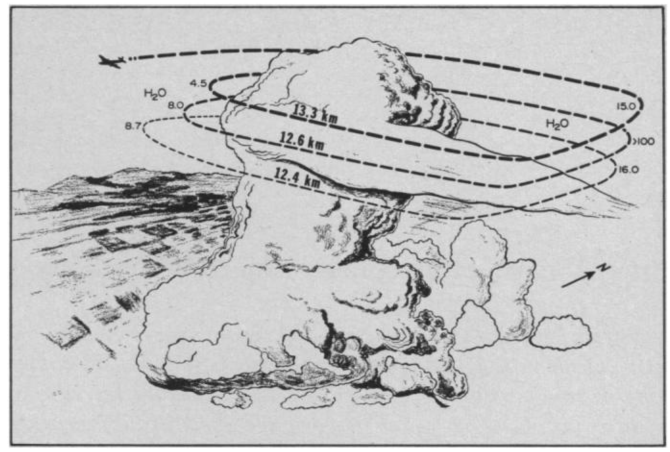

Fig. 1 (left). View of the Colorado thunderstorm cell from CV-990 (15 July 1971) looking to the north on an eastward traverse at an altitude of 12.6 km. The cell is 20.0 km from the aircraft. Fig. 2 (right). Flight paths around the Colorado thunderstorm cell. Section lines on the surface run south-north to the right on the illustration and east-west to the left. The water vapor mass is in units of 10^{-4} g cm^{-2}, and the altitudes are in kilometers.

15 July 1971 between 0000 and 0130 G.M.T. (Fig. 1). This experiment was conducted upstream, azimuth 280°, and downstream, azimuth 100°, of an isolated thunderstorm cell 150 km north-northeast of Denver, Colorado, at altitudes of 12.4, 12.6, and 13.3 km. The cell top is at 14.8 km. The tropopause averages approximately 13.3 km but is not clearly bounded. Mastenbrook (*3*) has emphasized that true stratospheric air in the summer over the west-central United States occurs principally above 16.0 km. The measurements we are discussing were made in the transitional or mixing zone at the base of the stratosphere.

In situ measurements of the temperature and the concentration of solid particles indicate that the CV-990 was just at the base of the stratosphere. Figure 2 illustrates the flight paths around this system from 0000 to 0130 G.M.T. The east-west tracks are approximately 80 km long, whereas the north-south tracks are on the order of 64 km long. The observations approximately spanned the life cycle of the cell system. In the three circumferential flight tracks, the mass of water vapor (in grams per square centimeter) above the flight level was considerably larger, as far as 20 km downstream of the cell, than upstream. Within the resolution accuracy of the radiometric inference system, at 45 km downstream the water vapor was again equivalent to the upstream mass at the end of the first traverse. The upstream values of water vapor mass (Fig. 1) are in general agreement with those reported by Mastenbrook (*4*).

The core of the cell moved approximately 15 km eastward during the total observation period of 90 minutes. For all three traverses the maximum downstream range at which excess water vapor mass above the aircraft could be detected approximated 45 km. One may assume that the residence time above flight level for the excess of thunderstorm water vapor above background water vapor within the limits of the radiometer sensitivity is 90 minutes. At this time only background concentrations of water vapor were detectable.

To further establish the validity of the radiometric inferences, we calculated saturation conditions and noted the presence or absence of cirrus clouds. If the entire mass of 16×10^{-4} g cm^{-2} of water vapor observed downstream and above the lower flight level of 12.4 km (Fig. 2) is contained in the column between 12.4 km and 14.8 km (the cell top), we calculate a mean water vapor mixing ratio of water vapor to air of 23 parts per million (ppm). Saturation conditions over ice for this column at a measured temperature of -73.0°C would require a mixing ratio of 43 ppm. In agreement with this calculation, no cirrus clouds were observed above the aircraft during the first pass.

During the second traverse of the cell at 12.6 km some 20 minutes later, the mixing ratio inferred from measurements of the mass of water vapor reached 110 ppm. This value is due to cirrus which remained above flight level during most of the traverse and resulted in a "false" water vapor mass. The 10.0- to 12.0-μm channel clearly indicated the presence of cirrus above. The last traverse around the cell was at 13.3 km. If the entire mass of water vapor measured above the aircraft, 15.0×10^{-4} g cm^{-2}, were concentrated in the column between 13.3 km, flight level, and 14.8 km, the cell top, saturation would just be reached. On this pass, cirrus occurrence approximately one-half of the time was consistent with the calculation. Restricting the layer to 14.8 km, the visible cell top, precludes any assumptions that the water vapor extends above the cloud top in the lower stratosphere and is an extreme case for saturation.

Before examining the mechanism for the vertical transport of water vapor by thunderstorms, we can summarize the mean water vapor mass upstream and downstream of the six cells studied. All of the cells penetrated the tropopause, and the water vapor masses were averaged at the highest flight levels ($\sim$13.3 km). The water vapor mass upstream of the cells averages 5.0×10^{-4} g cm^{-2}, whereas that downstream of the cells averages 16.0×10^{-4} g cm^{-2}, larger than the value upstream by a factor of 3. This increase was not measurable 45 km downstream of the cells.

Let us now consider a vertical transport mechanism in thunderstorms that increases the water vapor mass by 10×10^{-4} g cm^{-2} in a column above the downstream flight level of 12.4 km (Fig. 2). This total turbulent transport upward, Tr, assumed to continue for approximately 20 minutes, is given by

$$Tr = \rho W \bar{s} t = 10 \times 10^{-4} \text{ g cm}^{-2} \quad (7)$$

where ρ is the density (1.8×10^{-4} g cm^{-3}), $\bar{s}$ is the mixing ratio of water vapor to air (23.0 ppm or 23.0 g g^{-1}), and t is the time (1.2×10^3 seconds). Solving for W in Eq. 7, we obtain 2.0

m sec^{-1} for the vertical velocity over the 20-minute period. This velocity is consistent with previous values from thunderstorm research (*5*) for an average cell. Range height indication radar indicated a top growth rate of approximately 1.6 km in 20 minutes.

Thus we can speculate on the vertical mass transport of water vapor over larger areas into the upper troposphere and stratosphere. Thunderstorms east of Colorado reach much higher altitudes than storms in the Western Plains such as the storm discussed in detail, pushing well into the lower stratosphere. In addition, the tropopause is lower to the East during the thunderstorm season than in the Western Plains, and, as a result, there is a much higher stratospheric penetration in the East. Recently Lee and McPherson (*6*) reported on an observational survey of the tops of Oklahoma thunderstorms, stating that the tops of 469 thunderstorms exceeded 12.2 km during April, May, and June, 1967 through 1969. Of that number 33 percent exceeded 15.2 km. They (*6*) found the average base of the stratosphere during this period to be 12.2 km. On the other hand, only 25 percent of all Colorado thunderstorms penetrate into the stratosphere during the May-September thunderstorm season.

The Oklahoma thunderstorm statistics are at least typical for the eastern continental United States. If each of these approximately eight cells per day averages 10 km^2 and has a stratospheric injection of water vapor per cell of 20×10^{-4} g cm^{-2}, twice that of the drier Colorado storms, thunderstorms can transport vertically 1.6×10^9 g of water vapor per day into the Oklahoma stratosphere. Since the annual variability in the number of thunderstorms ranges from ½ to 1½ times the average number, we should consider this information when speculating on the effects of man-made additions of water vapor to the stratosphere. What finally happens to this injected water vapor remains an object for further study, as it may be swept out during the storm's dissipating stage.

P. M. Kuhn
M. S. Lojko
Environmental Research Laboratories, National Oceanic and Atmospheric Administration, Boulder, Colorado
E. V. Petersen
Airborne Science Office, National Aeronautics and Space Administration, Moffett Field, California 94035

References and Notes

1. P. M. Kuhn, *J. Atmos. Sci.* **27**, 937 (1970).
2. W. L. Smith, *Appl. Opt.* **9**, 1993 (1970).
3 H. J. Mastenbrook, personal communication.
4. ——, *J. Atmos. Sci.* **25**, 299 (1968).
5. H. R. Byers and R. R. Braham, Jr., *The Thunderstorm* (U.S. Weather Bureau, Washington, D.C., 1949).
6. J. T. Lee and A. McPherson, *Proceedings of the International Conference on Atmospheric Turbulence* (Royal Aeronautical Society, London, 1971), p. B1.
7. Work supported by the National Aeronautics and Space Administration, the Department of Transportation, and the National Oceanic and Atmospheric Administration.

17 August 1971

Martian Craters and a Scarp as Seen by Radar

Abstract. *Radar observations of Mars with a surface resolution of 1.3° in latitude and 0.8° in longitude have been carried out during the opposition of 1971. With a precision in surface height measurement approaching 75 meters in regions of high reflectivity, it has been possible to measure the detailed characteristics of a number of craters. Many of these can be identified with craters shown in Mariner photographs of Mars. In addition, a scarp has been seen at 41° west, 14° south with an average slope of about 6° extending over about 40 kilometers.*

As previously reported, radar has been applied during the oppositions of 1967 (*1*) and 1969 (*2, 3*) to determine directly the surface topography of Mars along the subearth trace. Those measurements, entirely restricted to the northern Martian hemisphere, disclosed a topographic variation from peak to valley of some 12 km. At a lateral surface resolution of 1.5° to 6° of longitude and a vertical resolution of several kilometers, little detail at the limit of resolution was seen. With the increased signal strength associated with the extremely favorable opposition of 1971, as well as with recent advances in instrumentation, it has been possible at the Haystack Observatory to make radar observations of the surface altitude of Mars with a precision often approaching 75 m. These observations have disclosed a wealth of detail concerning relatively small-scale topographic features such as surface craters and scarps.

In mid-July 1971, a series of thrice-weekly radar observations was begun. A phase-coded continuous wave (CW) waveform with an effective resolution (baud length) of 6 μsec was used. After reception, the echo signals were coherently integrated for 6.12 msec in the decoding analysis, yielding an effective detection bandwidth of approximately 160 hz. At the operating frequency of 7840 Mhz (3.8-cm wavelength) this choice of parameters provides a basic lateral surface resolution, if a spherical surface is assumed, of 1.3° in latitude and 0.8° in longitude. (The extent in longitude is less than in latitude because of the narrow band of Doppler frequencies passed by the finite detection bandwidth.) In many cases the surface scattering law further limits the region under observation. In a single night the rotation of Mars permits observation of only slightly more than 100° of longitude at the latitude of Haystack, because of the high southerly declinations characterizing the 1971 opposition. With observations made at intervals over a number of weeks, however, it has been possible to connect the topographic variation entirely around the planet at latitudes varying between −14.5° and −16.8° (*4*). A preliminary reduction of data obtained between 15 July and 10 August 1971 yields the variation in surface height shown in Fig. 1, a through c.

These data have not yet been compared with the results of the observations of 1967 and 1969 in an orbital fitting program. Thus, the reference altitude shown represents the mean of these observations and cannot yet be assigned an absolute radius. The closure at a longitude of 60° (*4*) and the derived ephemeris corrections (which varied smoothly over an interval of only 16 μsec for this series of observations) are here based on a comparison of data that differ in latitude by about 2° and extend over only a small band of common longitudes. Thus, a small systematic error may exist in these preliminary reductions (*5*); however, there is no significant effect on the detailed shapes of the major features that form the basis for this report.

A general conclusion from these results is that the overall topographic variation of some 15 km is similar to the total variation from peak to valley reported in northern latitudes (*2, 3*). The elevated region at 110° longitude in the northern latitudes still persists